https://doi.org/10.5194/egusphere-2026-1204
Preprint. Discussion started: 11 March 2026

Reconstructed VOC emissions reveal hidden ozone precursors: Overlooked roles of primary OVOCs and unmeasured species

Sijia Yin[1], Gan Yang[1], Chuang Li[1], Qingyan Fu[2], Juntao Huo[2], Yuruo Fu[1], Rengqi Yan[1], Lei Yao[1], Lin Wang[1,3,4,5]

[1] Shanghai Key Laboratory of Air Quality and Environmental Health, Department of Environmental Science & Engineering, Fudan University, Shanghai 200438, China;
[2] Shanghai Environmental Monitoring Center, Shanghai 200030, China;
[3] National Observations and Research Station for Wetland Ecosystems of the Yangtze Estuary, Shanghai 200438, China;
[4] IRDR International Center of Excellence on Risk Interconnectivity and Governance on Weather/Climate Extremes Impact and Public Health, Fudan University, Shanghai 200438, China;
[5] Shanghai Institute of Pollution Control and Ecological Security, Shanghai 200092, China

Correspondence to: Lin Wang (lin_wang@fudan.edu.cn)

Abstract. Ambient volatile organic compounds (VOCs), including non-methane hydrocarbons (NMHCs) and oxygenated VOCs (OVOCs), are critical precursors of tropospheric ozone (O_3). However, conventional estimates of ozone formation potential (OFP) derived from observed VOC concentrations may introduce substantial biases, as they neglect the photochemical degradation of primary VOCs and the concurrent generation of secondary OVOCs during atmospheric transport. This study quantified the sources of ambient OVOCs at a suburban site in Shanghai, China during summer 2020 to reconstruct their initial emission concentrations. Together with the reconstructed initial concentrations of NMHCs, we estimated the OFP of freshly emitted VOCs. In addition, the sources and OFP of unmeasured VOCs were inferred by concurrent measurements of missing OH reactivity. Our results demonstrate that photochemical reactions substantially altered the composition and source characteristics of VOCs, leading to pronounced discrepancies in OFP estimation between observed and reconstructed initial concentrations. Specifically, OFP contributions from reconstructed NMHCs (52.3%) were underestimated by 31.7% when derived from observed concentrations for this site, whereas those from reconstructed OVOCs (33.2%) were overestimated by 42.6%. Reconstructed VOC emissions indicated that anthropogenic sources dominated total emissions (71.5%), whereas OVOCs constituted a substantial fraction of total VOC emissions (40.8%). Unmeasured VOCs, primarily of biogenic origin, contributed an additional 12.6%. Collectively, OVOCs and unmeasured species exhibited OFP comparable to NMHCs, underscoring their critical role in O_3 production and the necessity of incorporating these species into the design of comprehensive and effective O_3 control strategies.

1 Introduction

As a critical group of precursors for ozone (O_3), atmospheric volatile organic compounds (VOCs), including non-methane hydrocarbons (NMHCs) and oxygenated VOCs (OVOCs), have attracted considerable attention in air pollution mitigation

https://doi.org/10.5194/egusphere-2026-1204
Preprint. Discussion started: 11 March 2026

strategies (Atkinson and Arey, 2003; Atkinson and Carter, 1984; Mellouki et al., 2015). To identify key O_3 precursors, the maximum incremental reactivity (MIR) method is widely applied to calculate the ozone formation potential (OFP) of VOCs (Gu et al., 2021; Huang et al., 2020; Ou et al., 2015; Wang et al., 2023). The MIR values - which reflect the mass change of O_3 per unit mass of VOCs added in the smog chambers or numerical simulations - are normally obtained based on the initial VOC concentrations (i.e., the concentrations in the fresh emissions before undergoing photochemical reactions) (Carter, 1994, 2010). However, studies about OFP of VOCs are mostly performed with observed VOC concentrations after atmospheric processing (Cui et al., 2022; Huang et al., 2020; Hui et al., 2023; Shang et al., 2022), which could introduce uncertainties in accurately identifying key precursors for ozone formation, as the degradation of NMHCs and the formation of secondary OVOCs during atmospheric transport can significantly alter compositions and concentrations of VOCs (Zheng and Xie, 2025).

While it is relatively straightforward to understand the photodegradation of NMHCs and trace back to their initial concentrations, it is less common to notice that ambient OVOCs are not only directly emitted from anthropogenic and biogenic sources, but also generated from photochemical oxidation of precursors (Huang et al., 2020; Ou et al., 2015). In other words, calculating OFP using observed OVOC concentrations could overestimate their true contributions unless the secondary fraction is excluded. An accurate source apportionment of primary and secondary OVOCs is thus essential for a reliable OFP estimation.

Commonly used VOC source appointment approaches, including principal component analysis, positive matrix factorization, and chemical mass balance, generally neglect the influence of photochemical reactions of VOCs during atmospheric transport, and thus could not effectively quantify the relative contributions of primary emissions and secondary sources. In contrast, the photochemical age-based parameterization method (PAPM) explicitly incorporates OH radical oxidation and photolysis of OVOCs (De Gouw et al., 2005, 2018), enabling a more precise quantification of their sources. While the PAPM has been widely applied to OVOC source apportionment in China (Huang et al., 2020; Li et al., 2024b), its application remains to a few OVOCs, such as formaldehyde, acetaldehyde, and acetone. The source distributions of other critical OVOCs are yet to be characterized (Li et al., 2024b).

In addition, a large number of VOCs remain undetected or unquantified by current analytical techniques, especially those with multifunctional groups or complex molecular structures (Spinelle et al., 2017; Wang et al., 2024b). These unmeasured VOCs can profoundly affect our understanding of VOC contributions to O_3 formation. For instance, Tan et al. (2019) reported that unmeasured species accounted for up to 60% of O_3 production and contributed nearly 50% to the total OH reactivity (R_{OH}) at a suburban site in Heshan, China. Other studies have shown that unmeasured VOCs resulted in up to a 46 % overestimation in the response of O_3 to nitrogen oxides (Wang et al., 2024b), and a 30% underestimation in simulated net O_3 production rates (Zhou et al., 2024). Collectively, these findings underscore the critical importance of unmeasured VOCs in accurately characterizing O_3 formation.

In this study, we applied the PAPM to quantify the contributions of anthropogenic and biogenic sources to 208 OVOCs measured at a suburban site of Shanghai, China from 1 August to 15 September 2020 (Yang et al., 2022). In addition, the

https://doi.org/10.5194/egusphere-2026-1204
Preprint. Discussion started: 11 March 2026

sources of unmeasured VOCs were inferred using measurements of missing R_{OH} combined with a multiple linear regression (MLR) approach. Based on the source apportionment results, the initial emission concentrations of OVOCs, NMHCs, and unmeasured VOCs were reconstructed to evaluate their OFP at the emission site, and to identify the key O_3 precursors and contributing sources.

2 Methods

2.1 Field campaign

A field campaign was carried out at the Dianshan Lake (DSL) Air Quality Monitoring Supersite (120.98°E, 31.09°N), Shanghai, China (Fig. S1). The sampling site is ~15 m above ground, and surrounded by farmland, vegetation, several villages, and Dianshan Lake. As a representative of the suburban environment, this site has been frequently selected as a reference site for the study of air pollution in the Yangtze River Delta region (Feng et al., 2023; Wu et al., 2023; Yang et al., 2022).

Table S1 summarizes the observed concentrations of VOCs. A gas chromatograph with mass spectrometry and flame ionization detection (hereinafter referred to as GC-MS/FID; TH-PKU 300B, Wuhan Tianhong Instrument Co. Ltd., China) was used to measure 56 Photochemical Assessment Monitoring Station (PAMS) compounds (including 29 alkanes, 10 alkenes, 16 aromatics, and acetylene) and 11 carbonyls (including 6 aldehydes and 5 ketones), a Kore proton transfer reaction time-of-flight mass spectrometry (KORE PTR 3C, KORE Technologies, UK) was used to measure formaldehyde and acetaldehyde, and a Vocus-2R PTR-TOF-MS (Vocus-PTR, Tofwerk AG and Aerodyne Research Inc., USA) was used to measure 57 NMHCs and 195 OVOCs without definitive identity assignments. In total, 321 VOCs (including 56 PAMS, 13 carbonyls, 57 unspecified NMHCs, and 195 unspecified OVOCs) were quantified in this campaign. Details of the instruments and their operation have been described previously (Yang et al., 2022).

Additionally, R_{OH} was measured using a comparative reactivity method (CRM) (Sinha et al., 2008) and calculated with measured inorganic and organic trace gas concentrations, respectively. In brief, pyrrole (C_4H_5N), used as a reference substance, was passed through a glass reactor and monitored by Vocus-PTR. OH radicals were then introduced to react with C_4H_5N, first in the presence of zero gas and then in the presence of ambient air. Comparing the concentration of C_4H_5N exiting the reactor with and without the ambient air allows determination of the measured OH reactivity (Sinha et al., 2008).

2.2 Photochemical age-based parameterization method

The PAPM assumes that the amount of each emitted OVOC is proportional to the amount of an inert tracer (e.g., acetylene/C_2H_2), and that reactions with OH radicals dominate the photochemical removal of OVOCs. In this method, ambient OVOC concentrations can be attribute to anthropogenic primary emissions, anthropogenic secondary formation, biogenic sources, and regional background, as expressed in Eq. (1):

https://doi.org/10.5194/egusphere-2026-1204
Preprint. Discussion started: 11 March 2026

$$[\mathrm{OVOC}] = \mathrm{ER}_{\mathrm{OVOC}} \times [\mathrm{C_2H_2}] \times \exp\left[-\left(k^*_{\mathrm{OVOC}} - k_{\mathrm{C_2H_2}}\right)[\mathrm{OH}]\Delta t_a\right] + \mathrm{ER}_{\mathrm{precursor}} \times [\mathrm{C_2H_2}] \times \frac{k_{\mathrm{precursor}}}{k^*_{\mathrm{OVOC}} - k_{\mathrm{precursor}}} \times \frac{\exp\left(-k_{\mathrm{precursor}}[\mathrm{OH}]\Delta t_a\right) - \exp\left(-k^*_{\mathrm{OVOC}}[\mathrm{OH}]\Delta t_a\right)}{\exp\left(-k_{\mathrm{C_2H_2}}[\mathrm{OH}]\Delta t_a\right)} + \mathrm{ER}_{\mathrm{biogenic}} \times [\mathrm{isoprene}]_{\mathrm{source}} + [\mathrm{background}] \quad (1)$$

where $\mathrm{ER}_{\mathrm{OVOC}}$ and $\mathrm{ER}_{\mathrm{precursor}}$ are the emission ratios of OVOC and their precursors to relative C_2H_2; k_{C2H2} and $k_{\mathrm{precursor}}$ are the OH rate coefficients of C_2H_2 and OVOC precursors, respectively; k^*_{OVOC} is the effective loss rate constant of OVOC representing the combined loss due to OH radicals and photolysis, for which the daytime photolysis of 13 carbonyls was considered in this study (Sect. S1 and Table S2); $[C_2H_2]$ is the observed concentration of acetylene; $\mathrm{ER}_{\mathrm{biogenic}}$ is the emission ratio of OVOCs to isoprene from biogenic emissions ($[\mathrm{Isoprene}]_{\mathrm{source}}$, calculated using Eq.(2)), and [background] denotes the background level. OH exposure of anthropogenic VOCs ($[\mathrm{OH}]\Delta t_a$) is calculated from a species ratio method using the observed ethylbenzene and m&p-xylene concentrations (Roberts et al., 1984).

Note that the consumption of VOCs is dominated by OH radicals during the daytime. Consequently, the sources of OVOCs observed during 07:00 to 18:00 local time were calculated using a least-squares fit as listed in Tables S3 and S4.

2.3 Estimation of initial VOCs

The photochemical loss of VOCs is dominated by reactions with OH radicals during the daytime, and other removal paths, including deposition and reactions with NO_3 radical or O_3, are regarded to be negligible. Thus, the initial concentration of NMHCs emitted from sources can be estimated by Eq. (2):

$$\left[\mathrm{NMHC}_{i,j}\right]_{\mathrm{source}} = \left[\mathrm{NMHCs}_{i,j}\right]_{\mathrm{t}} \times \exp\left(k_i[\mathrm{OH}]\Delta \mathrm{t}_j\right) \quad (2)$$

where $[\mathrm{VOC}_{i,j}]_{\mathrm{source}}$ is the initial concentration of NMHC species i from the j^{th} source; $[\mathrm{VOC}_{i,j}]_{\mathrm{t}}$ is the observed concentration of VOC species i from the j^{th} source (including anthropogenic and biogenic sources); $[\mathrm{OH}]\Delta t_j$ is the OH exposure of VOCs from the j^{th} source, whose detailed descriptions are provided in Sects. S2 and S3; and k_i is the OH rate constant of NMHC species i (Sect. S4 and Table S5). In this study, isoprene, monoterpenes ($C_{10}H_{16}$), and sesquiterpenes ($C_{15}H_{24}$) are classified as biogenic VOCs, whereas other NMHCs are categorized as anthropogenic VOCs.

Based on the source apportionment results (Sect. 3.1), the initial concentration of OVOCs can be estimated by Eq. (3).

$$\left[\mathrm{OVOC}_{i,j}\right]_{\mathrm{source}} = \mathrm{ER}_{i,j} \times \left[\mathrm{tracer}_j\right]_{\mathrm{source}} \quad (3)$$

where $\mathrm{ER}_{i,j}$ is the emission ratios of the OVOC species i relative to the initial tracer concentration from the j^{th} source ($[\mathrm{tracer}_j]_{\mathrm{source}}$, specifically $[C_2H_2]_{\mathrm{source}}$ for anthropogenic and $[\mathrm{isoprene}]_{\mathrm{source}}$ for biogenic source).

2.4 Estimation of unmeasured VOCs

The difference between measured R_{OH} and calculated R_{OH}, termed as missing R_{OH}, is a parameter for assessing the reactivity of unmeasured or unrecognized compounds.

https://doi.org/10.5194/egusphere-2026-1204
Preprint. Discussion started: 11 March 2026

$$\text{Missing } R_{\text{OH}} = \text{Measured } R_{\text{OH}} - \sum_i k_{(\text{X}_i+\text{OH})}[\text{X}_i] \quad (4)$$

where $[X_i]$ represents the observed concentration of inorganic or VOC species i, and $k_{(X_i+OH)}$ represents the first-order rate coefficient for the reaction of species i with OH radicals. To explore the potential sources of missing R_{OH}, we quantified the sources of missing R_{OH} by a MLR method introduced by Wang et al. (2024b).

$$\text{Missing } R_{\text{OH}} = a[\text{C}_2\text{H}_2] + b[\text{isoprene}]_{\text{source}} + c[\text{O}_x] + C_{\text{background}} \quad (5)$$

where $[O_x]$ is the observed concentrations of NO_2 + O_3. $C_{background}$ is interception. a, b, c, and $C_{background}$ are the fitted coefficients, which are 0.39 s^{-1} ppb^{-1}, 2.48 s^{-1} ppb^{-1}, 0.04 s^{-1} ppb^{-1}, and 2.27 s^{-1}, respectively.

Unmeasured VOCs, such as long-chain alkanes, diterpenes, and OVOCs with more than four oxygen atoms, are mainly derived from anthropogenic sources, biogenic sources, and secondary generation, respectively. These compounds exhibit high reactivity toward OH radicals and are therefore expected to be important sources of missing R_{OH} (Li et al., 2020; Wang et al., 2020; Wu et al., 2020). In addition to VOC species, other reactive gases such as hydrogen sulfide, HONO, and ammonia, etc., although not measured in this study, have been identified in previous studies as important contributors to total R_{OH} (Anglada and Solé, 2017; Pai et al., 2021; Wine et al., 1981). Moreover, heterogeneous OH uptake on atmospheric aerosol surfaces represents another non-negligible sink of OH radicals (Zhang et al., 2020), which may further contribute to missing R_{OH}. The background fraction of missing R_{OH} exhibited no correlations with anthropogenic or biogenic VOC emissions, nor with secondary formation. We therefore attributed the background fraction of missing R_{OH} to unmeasured inorganic reactive gases or unaccounted heterogeneous processes, and its OFP contribution was not considered in subsequent calculations. Missing R_{OH} associated with anthropogenic, biogenic, and secondary sources was attributed to unmeasured VOCs from the corresponding source. Given that unmeasured VOCs are likely a complex mixture of diverse chemical species, we scaled the concentrations of the 191 measured species with available MIR values (Table S5) from the corresponding source to compensate for missing R_{OH}, as shown in Eq. (6):

$$[\text{unmeasured VOC}_{i,j}]_t = [\text{VOC}_{i,j}]_t \times \frac{missing\ R_{OH,j}}{R_{OH,j}} \quad (6)$$

where $[\text{unmeasured VOCs}_{i,j}]_t$ denotes the concentrations of unmeasured VOC_i originating from the j^{th} source at the observation site, $[VOCs_{i,j}]_t$ represents the concentrations of measured VOCs from the j^{th} source at the observation site, missing $R_{OH,j}$ and $R_{OH,j}$ represents the OH reactivity of unmeasured and measured VOCs from the j^{th} source, respectively.

Based on the equivalent concentrations of measured VOCs, the initial concentrations of unmeasured VOCs, $[\text{unmeasured VOCs}_{i,j}]_{\text{source}}$, were estimated following the same approach as that for measured species in Sect. 2.3. Note that unmeasured VOCs associated with secondary formation were excluded from this calculation, as they represent secondary OVOCs. Accordingly, the initial unmeasured anthropogenic and biogenic VOCs were determined using Eq. (7), with the same source-specific OH exposures and corresponding OH rate constants as those used for measured species.

$$\left[\text{unmeasured VOCs}_{i,j}\right]_{\text{source}} = \left[\text{unmeasured VOCs}_{i,j}\right]_t \times \exp\left(k_i[\text{OH}]\Delta t_j\right) \quad (7)$$

https://doi.org/10.5194/egusphere-2026-1204
Preprint. Discussion started: 11 March 2026

2.5 Ozone formation potential

The MIR method was applied to calculate the OFP of individual VOC species (OFP_i) to evaluate their respective contributions to O_3 generation.

$$OFP_i = [VOC_i] \times MIR_i \quad (8)$$

where $[VOC_i]$ is the concentration of a species i and MIR_i is the maximum incremental reactivity coefficient for an individual species i, as reported by Carter et al. (2010). Note that MIR values are unavailable for many VOCs, particularly those detected by Vocus-PTR without structural information. To enable OFP estimation, MIR values for these species were assigned as follow: (1) If the molecular formula corresponds to a unique compound without isomers, the reported MIR value of that compound was directly assigned; (2) If the molecular formula matched multiple isomers, the minimum MIR value among multiple isomers was conservatively adopted; (3) Nevertheless, 130 OVOCs (Table S5), accounting for 7.8% of the total observed VOC concentration, still lacked MIR values. These species were excluded from both the OFP calculations and the estimation of unmeasured VOCs. Thus, we estimated the OFP of unmeasured VOCs with the equivalent concentrations and corresponding MIR coefficients of the 191 measured species with available MIR values. The MIR coefficients used for OFP estimation are summarized in Table S5.

These assignment strategies and the inference of unmeasured VOCs inevitably introduce uncertainties into the OFP calculations. A detailed discussion on the uncertainties associated with VOC measurements, k_{OH} and MIR assignments, and assumptions with unmeasured species is provided in Sect. S5, together with their impacts on the OFP estimation.

3 Results and discussion

3.1 Source apportionment of measured and unmeasured VOCs

Using the parametric method incorporating photochemical age, we quantified contributions of anthropogenic primary emissions, anthropogenic secondary formation, biogenic sources, and regional background during the daytime (07:00–18:00 local time) for 8 aldehydes, 5 ketones, and 195 unspecified OVOCs. The fitted results, as summarized in Tables S3 and S4, show a good agreement with observed concentrations (R = 0.40–0.90) and reconstruct the time series well, as illustrated for formaldehyde, acetaldehyde, and acetone in Fig. 1.

https://doi.org/10.5194/egusphere-2026-1204
Preprint. Discussion started: 11 March 2026

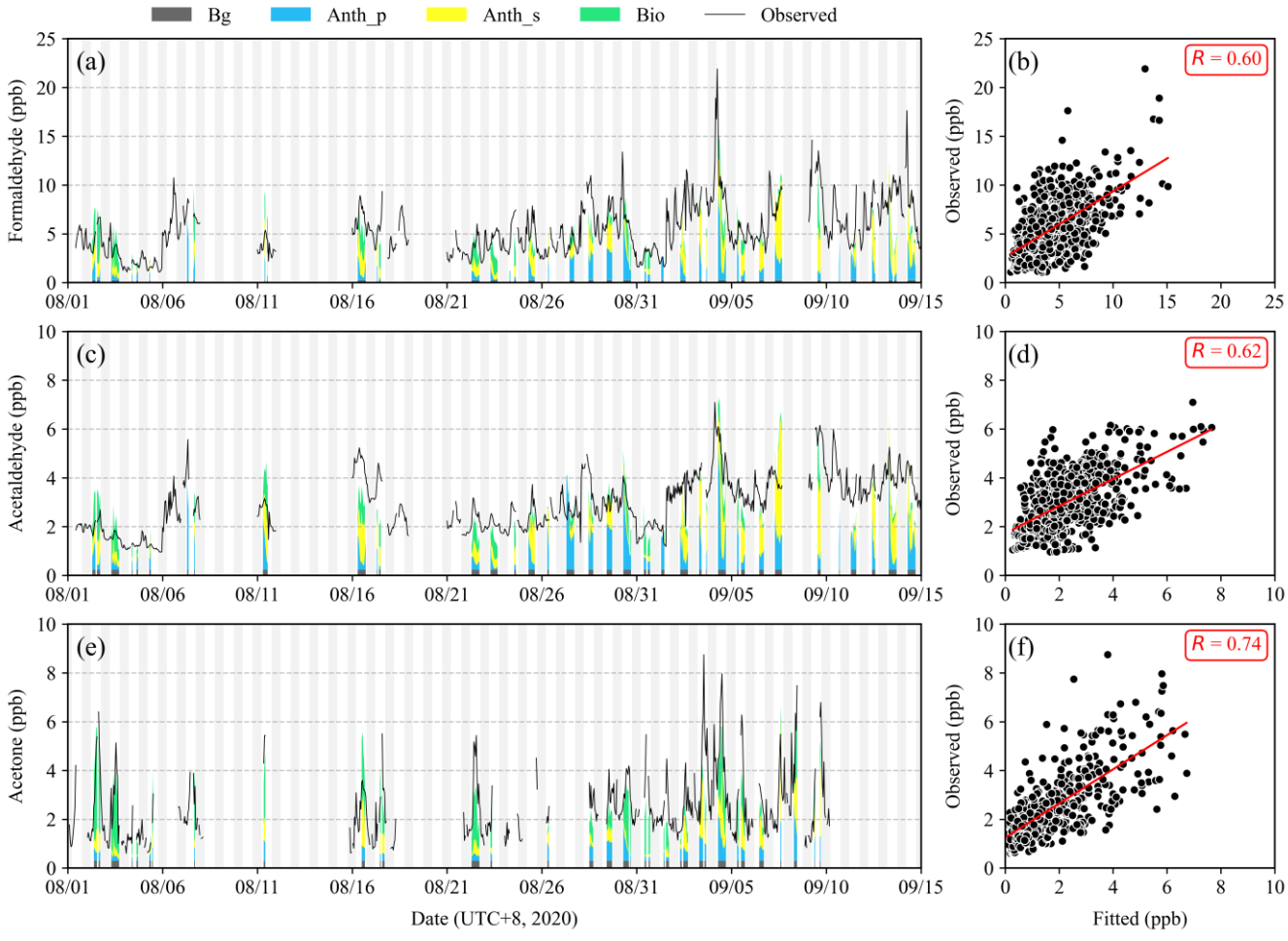

Figure 1. Time series (a, c, e) and scatter plot (b, d, f) of the fitting result versus the measured concentrations of formaldehyde, acetaldehyde, and acetone. Sources include anthropogenic primary emissions (Anth_p), anthropogenic secondary formation (Anth_s), biogenic sources (Bio), and background (Bg). Shaded areas in (a, c, e) represent nighttime, and missing data in (a, c, e) are due to the unavailability of tracer gases or OH exposure.

https://doi.org/10.5194/egusphere-2026-1204
Preprint. Discussion started: 11 March 2026

Ambient aldehydes, as shown in Fig. S2a, were predominantly of anthropogenic sources, with a large fraction of anthropogenic secondary formation (36.5%) and anthropogenic primary emissions (33.1%). Biogenic sources (24.7%) also played a notable role, whereas the regional background was minor (5.6%). Specifically, anthropogenic secondary formation was dominant for several major aldehydes, including formaldehyde (37.5%), acetaldehyde (36.0%), and propanal (34.6%). In contrast, biogenic sources were dominant for MACR (81.8%), pentanal (39.7%), hexanal (67.2%), butanal (52.1%), and acrolein (48.7%).

Ketones exhibited a higher regional background contribution (9.2%) compared to aldehydes (Fig. S2b). Biogenic sources represented the dominant source of ketones (47.1%), with particularly high contributions to MVK (69.0%), 2-pentanone (64.3%), 2-butanone (50.7%), and acetone (45.3%). Anthropogenic secondary formation (24.9%) and anthropogenic primary emissions (18.9%) were also important contributors. Collectively, our results underscore a substantial contribution of photochemically derived carbonyls from anthropogenic VOC precursors during daytime at the DSL site.

For unspecified OVOCs measured by Vocus-PTR, as shown in Fig. S2c, anthropogenic primary emissions accounted for the largest fraction (36.9%), followed by anthropogenic secondary formation (21.2%), biogenic sources (34.2%), and a low regional background level (7.7%). Specifically, $C_nH_{2n}O_2$ (n=2-8; likely alkanoic acids) were mainly emitted from primary anthropogenic activities (34.7-84.4%), such as traffic or agricultural sources (Mattila et al., 2018). Compounds such as $C_6H_{14}O_2$, $C_9H_{10}O$, $C_2H_3NO_2$, C_3H_7NO, C_5H_9NO, and $C_6H_5NO_3$ - likely representing solvents and amides emitted from industrial processes, volatile chemical products, or wildfire - were also primarily emitted from anthropogenic primary sources (> 50%) (Salvador et al., 2024; Zhang et al., 2024). OVOCs with more than or equal to three oxygen atoms (e.g., $C_2H_4O_3$, $C_4H_4O_3$, $C_4H_2O_4$, $C_5H_6O_3$, $C_4H_4O_4$, and $C_5H_4O_4$) were likely formed via multi-generation oxidation reactions of anthropogenic VOCs, with over 60% attributed to anthropogenic secondary formation. Biogenic sources were dominant sources of $C_nH_{2n}O$ (n=9-14), $C_8H_8O_2$, $C_9H_6O_2$, $C_8H_6O_3$, $C_{10}H_{14}O_2$, and $C_{10}H_{20}O_2$, accounting for 45.0-74.2%. These species likely represent carbonyls, fatty acid derivatives, and phenylpropanoids, commonly identified as primary biogenic OVOCs (Ma et al., 2022a; Wang et al., 2024a). In addition, several compounds such as C_6H_8O, $C_6H_8O_3$, $C_8H_{10}O_3$, $C_8H_6O_4$, $C_9H_{14}O_2$, $C_9H_{10}O_3$, $C_9H_8O_4$, $C_{10}H_8O_3$, $C_{12}H_{18}O$, and $C_{13}H_{12}O_2$ also exhibited substantial contributions from biogenic sources, ranging from 44.8% to 77.7%. These OVOCs have been identified as dominant products of terpene oxidation in laboratory simulations, and frequently observed in forest environments (Calogirou et al., 1999; Li et al., 2020; Vermeuel et al., 2023).

Unlike OVOCs, 113 NMHCs, including 29 alkanes, 9 alkenes, 16 aromatics, 1 alkyne, 3 terpenes, and 55 unspecified ones, are considered directly emitted since there is no secondary formation for NMHCs. Among them, isoprene, $C_{10}H_{16}$, and $C_{15}H_{24}$ are classified as biogenic VOCs, whereas the other 110 NMHCs are categorized as anthropogenic VOCs. It should be noted, however, that terpenoids may also be emitted from anthropogenic activities, such as vehicular exhaust and the usage of volatile chemical products (Borbon et al., 2001; Gu et al., 2024; Xie et al., 2025). Moreover, certain benzenoid compounds have been reported to be emitted from biogenic sources as well (Ma et al., 2022a; Misztal et al., 2015; Wang et

https://doi.org/10.5194/egusphere-2026-1204
Preprint. Discussion started: 11 March 2026

al., 2024a; Wohl et al., 2023). Nevertheless, the impact of these cross-sources was generally considered to be minor (Ma et al., 2022a; Seltzer et al., 2021).

In addition to the detected VOCs, numerous other VOCs are present in the ambient air but were not measured during this campaign. Those unmeasured VOCs led to a gap between the measured and calculated R_{OH}, i.e., missing R_{OH}. To explore the potential sources of missing R_{OH} at the DSL site, we quantified its sources by applying an MLR method. The fitted and calculated missing R_{OH} were in good agreement (R = 0.63, Fig. S3). The estimated missing R_{OH} is approximately 6.84 ± 4.41 s^{-1} during the daytime. Biogenic sources accounted for the largest fraction (2.36 ± 1.71 s^{-1}, 34.3%), followed by background (2.12 s^{-1}, 30.9%) and secondary sources (2.10 ± 1.37 s^{-1}, 30.5%). In contrast, anthropogenic sources played a minor role in missing R_{OH} (0.29 ± 0.20 s^{-1}, 4.2%). These results are consistent with previous suggestions that missing R_{OH} was mainly from biogenic sources or photochemical production processes (Di Carlo et al., 2004; Yang et al., 2017). To quantify the OFP of unmeasured VOCs, the missing R_{OH} attributed to anthropogenic, biogenic, and secondary sources was converted into equivalent concentrations of measured VOCs from corresponding sources using Eq. (6). The background fraction of missing R_{OH} was not converted, as it was attributed to undetected reactive inorganic gases or unaccounted heterogeneous reactions rather than unmeasured VOCs. Our results showed that unmeasured VOCs were dominated by secondary OVOCs (4.07 ± 2.55 ppbv, 43.8%) during daytime, followed by biogenic VOCs (3.72 ± 2.46 ppbv, 40.1%) and anthropogenic VOCs (1.49 ± 1.00 ppbv, 16.0%).

3.2 VOC evolution from initial emission to observation

Based on the above calculation, as shown in Fig. 2a, the daytime average concentration of total VOCs (TVOCs, including measured and unmeasured VOC species) at the observation site was estimated to be 58.35 ± 24.18 ppbv. Among them, measured species were 49.07 ± 21.34 ppbv. Measured OVOCs were the dominant group (52.4%), with unspecified OVOCs comprising the largest fraction (26.4%), followed by aldehydes (17.2%) and ketones (8.8%). Measured NMHCs contributed 31.7% of TVOCs, with alkanes as the major fraction (17.7%), followed by unspecified NMHCs (4.0%), alkenes (3.2%), aromatics (3.2%), terpenes (2.4%), and alkynes (1.3%). In addition, the daytime average concentration of unmeasured VOCs at the observation site was estimated to be equivalent to 9.28 ± 5.22 ppbv of measured VOCs, which contributed approximately 15.9% of TVOCs.

Source apportionment reveals that anthropogenic primary sources were the largest contributors to TVOCs at the observation site (48.9%), followed by biogenic sources (26.2%), anthropogenic secondary formation (21.0%), and regional background (3.8%). This distribution reflects a substantial anthropogenic influence, consistent with nearby urban and traffic emissions at the DSL site, although contributions from biogenic sources were also evident.

After deducting secondary formation contributions and accounting for photochemical aging, the initial concentration of individual measured VOCs was estimated (Table S5). In addition, the initial concentration of unmeasured VOCs was estimated using Eq. (7) based on the equivalent observed concentrations of measured VOCs. As shown in Fig. 2b, the estimated daytime average initial concentration of TVOCs was 47.71 ± 22.64 ppbv. Among these, measured species were

https://doi.org/10.5194/egusphere-2026-1204
Preprint. Discussion started: 11 March 2026

41.71 ± 19.79 ppbv. In contrast to the distribution at the observation site, NMHCs (22.25 ± 18.39 ppbv, 46.6%) constituted the largest fraction of the initial TVOCs, rather than OVOCs (19.46 ± 9.76 ppbv, 40.8%). Based on Eq. (7), the initial concentration of unmeasured VOCs was estimated to be 6.00 ± 3.56 ppbv, accounting for 12.6% of initial TVOCs.

Anthropogenic and biogenic source emissions contributed 71.5% and 28.5% of initial TVOCs, respectively. A notable feature of these emissions is the substantial presence of OVOCs in primary sources. Anthropogenic OVOCs alone contributed 24.1% of the initial TVOCs, indicating that a considerable fraction of oxygenated compounds originated directly from anthropogenic activities. Biogenic emissions also contained a large proportion of OVOCs, representing more than half of the total biogenic VOCs. These findings are consistent with bottom-up emission inventories (Gu et al., 2021; Ou et al., 2015; Salvador et al., 2024; Yan et al., 2024), as well as direct source measurements (Li et al., 2024a; Sekimoto et al., 2023; Seltzer et al., 2021; Wang et al., 2024a), which have reported significant primary OVOC emissions from solvents, industrial activities, volatile chemical products, and plant emissions. Concentrations of primarily emitted OVOCs were comparable to those of NMHCs. However, previous studies mainly focused on NMHCs and neglected the role of primarily emitted OVOCs (Ma et al., 2022b).

Comparison between initial and observed VOCs reveals a substantial compositional change during atmospheric transport. The concentration of TVOCs at the observation site was 10.64 ppbv (22.3%) higher than the initial TVOCs. However, NMHC concentrations were underestimated by 16.8%. Species with the largest discrepancies were alkenes and aromatics: the average initial concentrations of alkenes and aromatics were 3.13 ± 1.72 ppbv and 2.45 ± 1.80 ppbv, respectively, significantly exceeding their respective measured concentrations of 1.84 and 1.87 ppbv at the observation site. This discrepancy can be primarily attributed to the high reactivity of these compounds and thus their rapid photochemical degradation during atmospheric transport. OVOC concentrations, if inferred from observation, were overestimated by 57.1%. For instance, unspecified OVOCs increased from 10.21 ± 5.11 ppbv at the real emission to 15.39 ± 12.23 ppbv at the observation site, reflecting substantial secondary production during transport.

Photochemical aging also altered different sources' contributions to VOCs significantly. Anthropogenic and biogenic sources emitted 71.5% and 28.5% of TVOCs, respectively. However, anthropogenic primary VOCs only accounted for 48.9% of TVOCs when transported to the observation site. Photochemically degradable VOCs were converted into OVOCs, with these secondary products accounting for 21.1% of TVOCs at the observation site, explaining the increase of OVOCs from the real emission to ambient measurements.

https://doi.org/10.5194/egusphere-2026-1204
Preprint. Discussion started: 11 March 2026

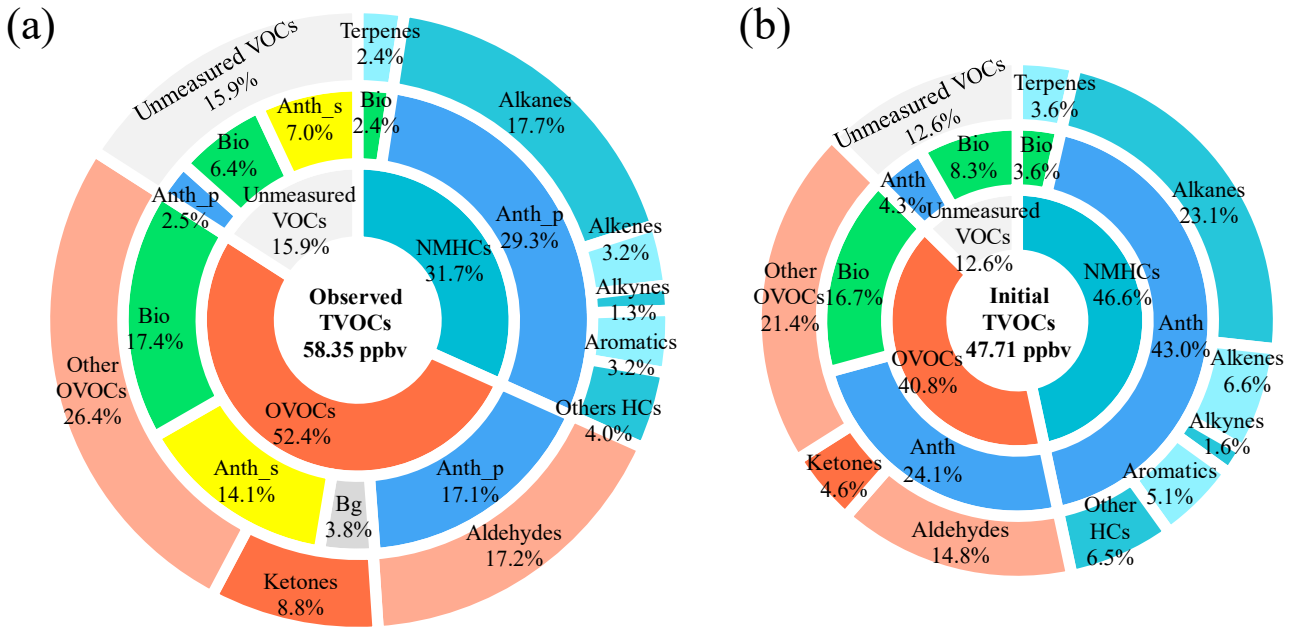

Figure 2. The contributions of different VOC groups and sources to (a) observed TVOCs at the observation site and (b) initial TVOCs at the emission site. The inner, middle, and outer rings represent the proportion of different VOC components, different sources, and different VOC groups to TVOCs, respectively. The size of the ring is proportional to TVOC concentrations.

3.3 Ozone formation potential and the key contributors

To identify key O_3 precursors, we further calculated the OFP of individual VOCs using the MIR method (Table S5). As shown in Fig. 3, the total OFP (TOFP) of TVOCs at the emission site was 431.96 ± 319.19 μg m^{-3}. Measured NMHCs contributed the largest fraction (52.3%), led by aromatics (12.6%), terpenes (12.6%), alkenes (12.5%), unspecified NMHCs (7.7%), alkanes (6.6%), and alkynes (0.2%). These results differed remarkably from those based on the observed concentrations, i.e., the OFP of measured NMHCs was smaller by 31.7% due to photochemical degradation. For instance, the OFP of initial alkenes was 54.11 ± 29.61 μg m^{-3}, but would be underestimated by 44.7% (29.95 ± 16.38 μg m^{-3}) if photochemical losses were not considered.

OVOCs are often regarded as secondary oxidation products and overlooked as primary O_3 precursors. However, our results demonstrate that directly emitted OVOCs accounted for 33.2% of initial TOFP, primarily from aldehydes (22.2%) and unspecified OVOCs (9.4%), whereas ketones contributed only 1.6%. It should be noted that the actual contribution of OVOCs was likely larger, as many OVOCs (with a total initial concentration of 3.2 ppbv, accounting for 6.7% of the initial TVOCs) were excluded from the OFP calculation because their MIR coefficients were unavailable. These findings show that primary OVOCs have an O_3 formation impact comparable to or exceeding that of many NMHCs. On the other hand, when

https://doi.org/10.5194/egusphere-2026-1204
Preprint. Discussion started: 11 March 2026

297 estimated directly from the observed concentrations, OVOCs' contributions to TOFP were overestimated by 42.6%, with
298 unspecified OVOCs in particular being overestimated by more than 50%, which is a bias largely attributable to secondary
299 production. This explains why, despite an underestimation of NMHCs' OFP, TOFP calculated from the observed TVOCs'
300 concentrations, i.e., 476.91 μg m^{-3} (Fig. 3a), was still 10.4% higher than that (431.96 μg m^{-3}) derived from the reconstructed
301 initial concentrations (Fig. 3b). These numbers highlight systematic biases introduced by photochemical aging and
302 underscore the necessity of reconstructing initial VOC emissions for accurate OFP assessments.
303 The contributions of unmeasured VOCs to TOFP were also considerable. The OFP of initial unmeasured VOCs was 62.77 ±
304 37.62 μg m^{-3}, representing 14.5% of initial TOFP, mainly contributed by unmeasured biogenic VOCs (46.51 ± 30.19 μg
305 m^{-3},10.8%), followed by unmeasured anthropogenic VOCs (16.26 ± 11.96 μg m^{-3}, 3.8%). Although their exact identities
306 remain to be elucidated, unmeasured VOCs' substantial OFP demonstrates that they are a non-negligible fraction of the O_3
307 precursors. Ignoring unmeasured VOCs would underestimate VOC's contributions to O_3 pollution.

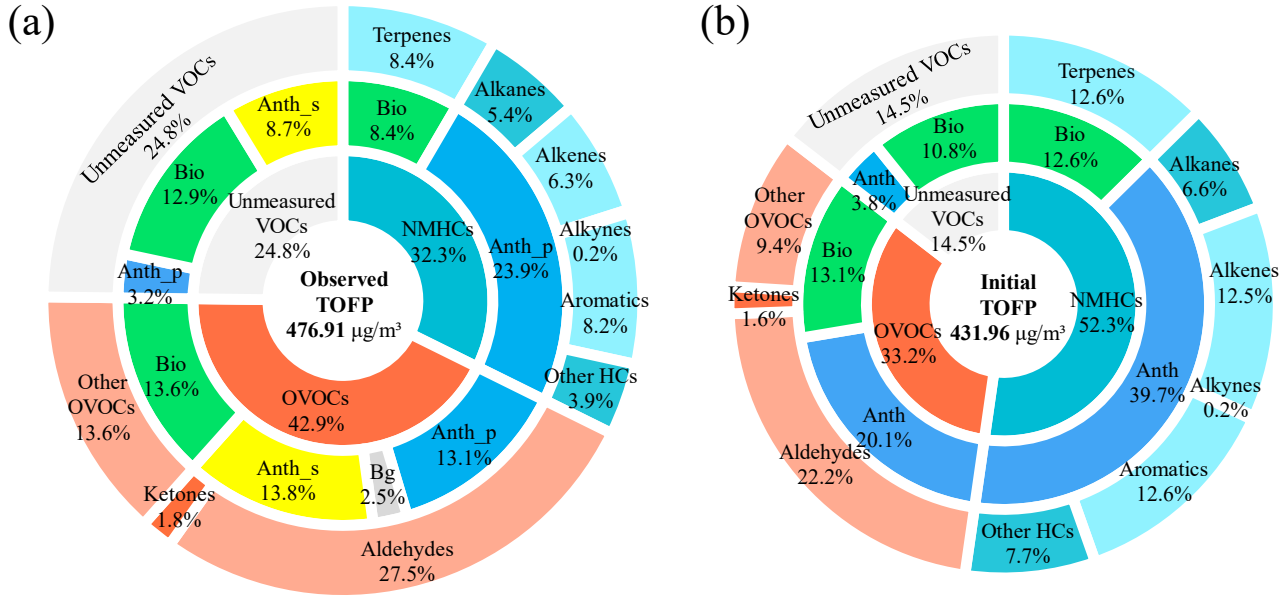

308

309 **Figure 3.** The contributions of different VOC groups and sources to TOFP (a) at the observation site and (b) at the emission
310 site. The inner, middle, and outer rings represent the proportion of different VOC components, different sources, and
311 different VOC groups to TOFP, respectively. The size of the ring is proportional to the total OFP.

312 In terms of individual VOCs at the emission site, formaldehyde was the largest single contributor to TOFP (13.4%),
313 consistent with emission inventory findings in Beijing and Guangzhou, China (Huang et al., 2021; Wang et al., 2023).
314 Isoprene ranked second (8.1%), which is emitted primarily from biogenic sources with a high photochemical reactivity.
315 Acetaldehyde was the third contributor (6.9%), largely driven by its relatively high concentrations (2.29 ± 1.43 ppbv). Other
316 key VOCs with high OFP included propylene, m&p-xylene, monoterpenes, ethylene, toluene, n-hexane, and o-xylene, each

https://doi.org/10.5194/egusphere-2026-1204
Preprint. Discussion started: 11 March 2026

accounting for more than 1.5% of TOFP (Fig. 4). The relative importance of these species differed notably from what is based on the observed concentrations (Fig. S4), particularly for propylene and n-hexane, which ranked the fourth and the tenth, respectively, based on their initial concentrations, but decreased to the seventh and the fifteenth when ranked by observed concentrations. This indicates that evaluations without considering initial concentrations could miss key O_3 precursors.

The top ten VOCs collectively accounted for 55.3% of TOFP, despite representing only 31.2% of initial TVOCs, highlighting that high OFPs did not necessarily correlate with high concentrations. For instance, $C_2H_4O_2$ (likely acetic acid), acetone, and ethane together comprised 12.1% of initial TVOCs but contributed only 1.2% to TOFP. Among the top ten contributors, eight species were primarily emitted from anthropogenic sources, reinforcing the dominant role of anthropogenic activities in O_3 formation in the suburban area of Shanghai.

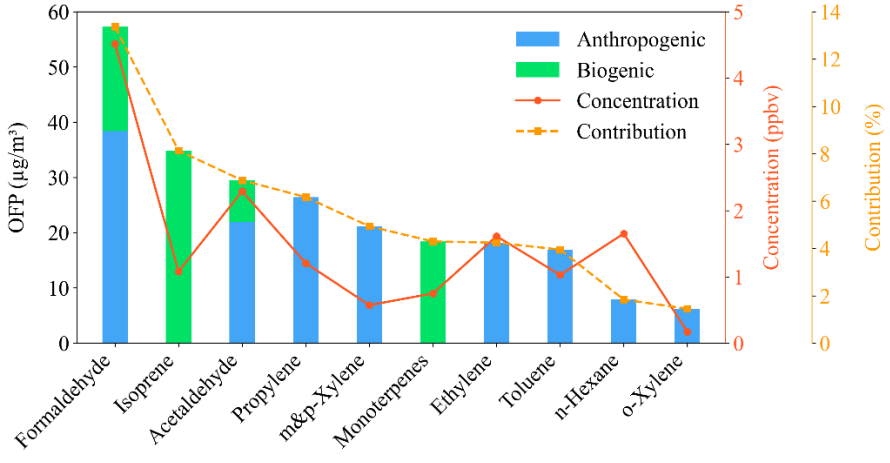

Figure 4. The initial concentrations and contributions of the top-ten OFP contributors during the daytime.

Anthropogenic emissions, including both measured and unmeasured species, have the potential to form about 274.42 ± 128.57 μg m^{-3} of O_3, accounting for 63.5% of TOFP. Initial anthropogenic NMHCs were the dominant contributors (39.7%) to TOFP, followed by anthropogenic OVOCs (20.1%), whereas unmeasured anthropogenic VOCs also represented a non-negligible fraction (3.8%). Formaldehyde, propylene, and acetaldehyde were the top three contributors among anthropogenic VOCs, which cumulatively contributed 20.1% of TOFP, even though they accounted for only 12.4% of initial TVOC concentrations. Initial biogenic VOCs had the potential to form about 157.54 ± 111.89 μg m^{-3} of O_3 (36.5% of TOFP), with biogenic OVOCs, terpenes, and unmeasured biogenic species contributing 13.1%, 12.6%, and 10.8% to TOFP, respectively. Isoprene, monoterpenes, and formaldehyde were the dominant biogenic contributors, with contributions of 8.1%, 4.3%, and 4.4%, respectively, mainly attributed to their abundant initial concentrations combined with their high MIRs.

https://doi.org/10.5194/egusphere-2026-1204
Preprint. Discussion started: 11 March 2026

4 Atmospheric implications

An accurate OFP estimation of VOCs is essential for designing effective O_3 pollution control strategies, particularly across the VOC-limited regimes of the Yangtze River Delta (Ren et al., 2022). However, ambient VOC measurements inherently represent photochemically processed mixtures rather than true emissions, complicating the identification of key O_3 contributors. This study demonstrates that photochemical aging substantially reshapes both the chemical composition and source characteristics of VOCs, systematically leading to underestimation of NMHCs and overestimation of OVOCs when relying solely on observed concentrations. Therefore, a reconstruction of initial emissions is necessary to correctly diagnose O_3 precursors.

By reconstructing initial VOC emissions from ambient observations, we provide observationally constrained evidence that primary OVOCs constitute a large fraction of total VOC emissions (40.8%) during our campaign, and that both anthropogenic and biogenic activities directly emit reactive oxygenated species with OFP comparable to NMHCs. These results help reconcile previous discrepancies between field observations, emission inventories, and source measurements by demonstrating that OVOCs are important O_3 precursors. Moreover, the substantial contribution of unmeasured VOCs (14.5% of total OFP) underscores the limitations of current monitoring networks, particularly for biogenic and oxygenated species. Thus, expanding measurement capabilities is critical for capture the true O_3 formation capacity of the atmosphere.

Current emission control strategies remain narrowly focused on a limited set of NMHCs (e.g., PAMS species) (Gao et al., 2025), which leaves a substantial portion of O_3 formation unmitigated when primary OVOCs and unmeasured species are overlooked. Our findings underscore the necessity of integrating these species into emission inventories, routine monitoring networks, and regional chemical transport models to improve the accuracy of O_3 predictions. On the other hand, given that these findings are based on observations from a single suburban site in Shanghai during summer, the spatial and seasonal representativeness of these results are inherently limited. Future investigations across diverse geographical regions and seasons are therefore warranted to evaluate the broader applicability of these conclusions. Consequently, by clarifying the OFP of a broader range of VOCs, this work supports a shift toward reactivity-based VOC management and provides an integrated observational–diagnostic framework that bridges ambient measurements with source emissions, offering a more robust solution for effective O_3 mitigation strategies.

https://doi.org/10.5194/egusphere-2026-1204
Preprint. Discussion started: 11 March 2026

Data availability

The data of this study are included in the article (and its Supplementary Material) and are available at https://doi.org/10.5281/zenodo.18932275 (Yin, 2026).

Supplement

The supplement related to this article is available online.

Author contributions

SY, conceptualization, methodology, investigation, formal analysis, data curation, visualization, writing–original draft, and editing; GY, QF, and JH, conducted the filed measurement; CL, YF, and RY, editing; LW, conceptualization, methodology, funding acquisition, project administration, supervision, and editing.

Competing interests

The contact author has declared that none of the authors has any competing interests.

Financial support

This work was financially supported by the National Natural Science Foundation of China (21925601 and 22127811).

https://doi.org/10.5194/egusphere-2026-1204
Preprint. Discussion started: 11 March 2026

References

Anglada, J. M. and Solé, A.: The Atmospheric Oxidation of HONO by OH, Cl, and ClO Radicals, J. Phys. Chem. A, 121, 9698–9707, https://doi.org/10.1021/acs.jpca.7b10715, 2017.

Atkinson, R. and Arey, J.: Atmospheric Degradation of Volatile Organic Compounds, Chem. Rev., 103, 4605–4638, https://doi.org/10.1021/cr0206420, 2003.

Atkinson, R. and Carter, W. P. L.: Kinetics and mechanisms of the gas-phase reactions of ozone with organic compounds under atmospheric conditions, Chem. Rev., 84, 437–470, https://doi.org/10.1021/cr00063a002, 1984.

Borbon, A., Fontaine, H., Veillerot, M., Locoge, N., Galloo, J. C., and Guillermo, R.: An investigation into the traffic-related fraction of isoprene at an urban location, Atmos. Environ., 35, 3749–3760, https://doi.org/10.1016/S1352-2310(01)00170-4, 2001.

Calogirou, A., Larsen, B. R., and Kotzias, D.: Gas-phase terpene oxidation products: a review, Atmos. Environ., 33, 1423–1439, https://doi.org/10.1016/S1352-2310(98)00277-5, 1999.

Carter, W. P.: Development of ozone reactivity scales for volatile organic compounds, Air Waste, 44, 881–899, 1994.

Carter, W. P.: Development of the SAPRC-07 chemical mechanism, Atmos. Environ., 44, 5324–5335, 2010.

Cui, L., Wu, D., Wang, S., Xu, Q., Hu, R., and Hao, J.: Measurement report: Ambient volatile organic compound (VOC) pollution in urban Beijing: characteristics, sources, and implications for pollution control, Atmospheric Chem. Phys., 22, 11931–11944, https://doi.org/10.5194/acp-22-11931-2022, 2022.

De Gouw, J., Middlebrook, A., Warneke, C., Goldan, P., Kuster, W., Roberts, J., Fehsenfeld, F., Worsnop, D., Canagaratna, M., Pszenny, A., and others: Budget of organic carbon in a polluted atmosphere: Results from the New England Air Quality Study in 2002, J. Geophys. Res. Atmospheres, 110, D16, 2005.

De Gouw, J., Gilman, J., Kim, S.-W., Alvarez, S., Dusanter, S., Graus, M., Griffith, S., Isaacman-VanWertz, G., Kuster, W., Lefer, B., and others: Chemistry of volatile organic compounds in the Los Angeles Basin: Formation of oxygenated compounds and determination of emission ratios, J. Geophys. Res. Atmospheres, 123, 2298–2319, 2018.

Di Carlo, P., Brune, W. H., Martinez, M., Harder, H., Lesher, R., Ren, X., Thornberry, T., Carroll, M. A., Young, V., Shepson, P. B., Riemer, D., Apel, E., and Campbell, C.: Missing OH Reactivity in a Forest: Evidence for Unknown Reactive Biogenic VOCs, Science, 304, 722–725, https://doi.org/10.1126/science.1094392, 2004.

Feng, J., Ren, E., Hu, M., Fu, Q., Duan, Y., Huang, C., Zhao, Y., and Wang, S.: Budget of atmospheric nitrous acid (HONO) during the haze and clean periods in Shanghai: Importance of heterogeneous reactions, Sci. Total Environ., 900, 165717, https://doi.org/10.1016/j.scitotenv.2023.165717, 2023.

Gao, Y., Wang, H., Zhu, S., Jing, S., Wang, Q., Huang, D. D., Li, Y., Lou, S., Fu, Q., Huang, C., and Su, H.: More Complete Reactive Organic Gases Measurements Reveal Greater Role of Combustion Emissions in Shanghai Megacity, J. Geophys. Res. Atmospheres, 130, e2024JD043129, https://doi.org/10.1029/2024JD043129, 2025.

Gu, S., Guenther, A., and Faiola, C.: Effects of Anthropogenic and Biogenic Volatile Organic Compounds on Los Angeles

https://doi.org/10.5194/egusphere-2026-1204
Preprint. Discussion started: 11 March 2026

Air Quality, Environ. Sci. Technol., 55, 12191–12201, https://doi.org/10.1021/acs.est.1c01481, 2021.

Gu, S., Luo, W., Charmchi, A., McWhirter, K. J., Rosenstiel, T., Pankow, J., and Faiola, C. L.: Limonene Enantiomeric Ratios from Anthropogenic and Biogenic Emission Sources, Environ. Sci. Technol. Lett., 11, 130–135, https://doi.org/10.1021/acs.estlett.3c00794, 2024.

Huang, X.-F., Zhang, B., Xia, S.-Y., Han, Y., Wang, C., Yu, G.-H., and Feng, N.: Sources of oxygenated volatile organic compounds (OVOCs) in urban atmospheres in North and South China, Environ. Pollut., 261, 114152, https://doi.org/10.1016/j.envpol.2020.114152, 2020.

Huang, Z., Zhong, Z., Sha, Q., Xu, Y., Zhang, Z., Wu, L., Wang, Y., Zhang, L., Cui, X., Tang, M., Shi, B., Zheng, C., Li, Z., Hu, M., Bi, L., Zheng, J., and Yan, M.: An updated model-ready emission inventory for Guangdong Province by incorporating big data and mapping onto multiple chemical mechanisms, Sci. Total Environ., 769, 144535, https://doi.org/10.1016/j.scitotenv.2020.144535, 2021.

Hui, L., Feng, X., Yuan, Q., Chen, Y., Xu, Y., Zheng, P., Lee, S., and Wang, Z.: Abundant oxygenated volatile organic compounds and their contribution to photochemical pollution in subtropical Hong Kong, Environ. Pollut., 335, 122287, https://doi.org/10.1016/j.envpol.2023.122287, 2023.

Li, H., Riva, M., Rantala, P., Heikkinen, L., Daellenbach, K., Krechmer, J. E., Flaud, P.-M., Worsnop, D., Kulmala, M., Villenave, E., Perraudin, E., Ehn, M., and Bianchi, F.: Terpenes and their oxidation products in the French Landes forest: insights from Vocus PTR-TOF measurements, Atmospheric Chem. Phys., 20, 1941–1959, https://doi.org/10.5194/acp-20-1941-2020, 2020.

Li, K., Zhang, J., Bell, D. M., Wang, T., Lamkaddam, H., Cui, T., Qi, L., Surdu, M., Wang, D., Du, L., El Haddad, I., Slowik, J. G., and Prevot, A. S. H.: Uncovering the dominant contribution of intermediate volatility compounds in secondary organic aerosol formation from biomass-burning emissions, Natl. Sci. Rev., 11, nwae014, https://doi.org/10.1093/nsr/nwae014, 2024a.

Li, Z.-J., He, L.-Y., Ma, H.-N., Peng, X., Tang, M.-X., Du, K., and Huang, X.-F.: Sources of atmospheric oxygenated volatile organic compounds in different air masses in Shenzhen, China, Environ. Pollut., 340, 122871, https://doi.org/10.1016/j.envpol.2023.122871, 2024b.

Ma, M., Gao, Y., Ding, A., Su, H., Liao, H., Wang, S., Wang, X., Zhao, B., Zhang, S., Fu, P., Guenther, A. B., Wang, M., Li, S., Chu, B., Yao, X., and Gao, H.: Development and Assessment of a High-Resolution Biogenic Emission Inventory from Urban Green Spaces in China, Environ. Sci. Technol., 56, 175–184, https://doi.org/10.1021/acs.est.1c06170, 2022a.

Ma, W., Feng, Z., Zhan, J., Liu, Y., Liu, P., Liu, C., Ma, Q., Yang, K., Wang, Y., He, H., Kulmala, M., Mu, Y., and Liu, J.: Influence of photochemical loss of volatile organic compounds on understanding ozone formation mechanism, Atmospheric Chem. Phys., 22, 4841–4851, https://doi.org/10.5194/acp-22-4841-2022, 2022b.

Mattila, J. M., Brophy, P., Kirkland, J., Hall, S., Ullmann, K., Fischer, E. V., Brown, S., McDuffie, E., Tevlin, A., and Farmer, D. K.: Tropospheric sources and sinks of gas-phase acids in the Colorado Front Range, Atmospheric Chem. Phys., 18, 12315–12327, https://doi.org/10.5194/acp-18-12315-2018, 2018.

https://doi.org/10.5194/egusphere-2026-1204
Preprint. Discussion started: 11 March 2026

Mellouki, A., Wallington, T. J., and Chen, J.: Atmospheric Chemistry of Oxygenated Volatile Organic Compounds: Impacts on Air Quality and Climate, Chem. Rev., 115, 3984–4014, https://doi.org/10.1021/cr500549n, 2015.

Misztal, P. K., Hewitt, C. N., Wildt, J., Blande, J. D., Eller, A. S. D., Fares, S., Gentner, D. R., Gilman, J. B., Graus, M., Greenberg, J., Guenther, A. B., Hansel, A., Harley, P., Huang, M., Jardine, K., Karl, T., Kaser, L., Keutsch, F. N., Kiendler-Scharr, A., Kleist, E., Lerner, B. M., Li, T., Mak, J., Nölscher, A. C., Schnitzhofer, R., Sinha, V., Thornton, B., Warneke, C., Wegener, F., Werner, C., Williams, J., Worton, D. R., Yassaa, N., and Goldstein, A. H.: Atmospheric benzenoid emissions from plants rival those from fossil fuels, Sci. Rep., 5, 12064, https://doi.org/10.1038/srep12064, 2015.

Ou, J., Zheng, J., Li, R., Huang, X., Zhong, Z., Zhong, L., and Lin, H.: Speciated OVOC and VOC emission inventories and their implications for reactivity-based ozone control strategy in the Pearl River Delta region, China, Sci. Total Environ., 530–531, 393–402, https://doi.org/10.1016/j.scitotenv.2015.05.062, 2015.

Pai, S. J., Heald, C. L., and Murphy, J. G.: Exploring the Global Importance of Atmospheric Ammonia Oxidation, ACS Earth Space Chem., 5, 1674–1685, https://doi.org/10.1021/acsearthspacechem.1c00021, 2021.

Ren, J., Guo, F., and Xie, S.: Diagnosing ozone–NO_x–VOC sensitivity and revealing causes of ozone increases in China based on 2013–2021 satellite retrievals, Atmospheric Chem. Phys., 22, 15035–15047, https://doi.org/10.5194/acp-22-15035-2022, 2022.

Roberts, J. M., Fehsenfeld, F. C., Liu, S. C., Bollinger, M. J., Hahn, C., Albritton, D. L., and Sievers, R. E.: Measurements of aromatic hydrocarbon ratios and NOx concentrations in the rural troposphere: Observation of air mass photochemical aging and NOx removal, Atmos. Environ., 18, 2421–2432, 1984.

Salvador, C. M. G., Wood, J. D., Cochran, E. G., Seubert, H. A., Kamplain, B. D., Overby, S. S., Birdwell, K. R., Gu, L., and Mayes, M. A.: Extreme Heat and Wildfire Emissions Enhance Volatile Organic Compounds: Insights on Future Climate, EGUsphere, 1–28, https://doi.org/10.5194/egusphere-2024-1808, 2024.

Sekimoto, K., Coggon, M. M., Gkatzelis, G. I., Stockwell, C. E., Peischl, J., Soja, A. J., and Warneke, C.: Fuel-Type Independent Parameterization of Volatile Organic Compound Emissions from Western US Wildfires, Environ. Sci. Technol., 57, 13193–13204, https://doi.org/10.1021/acs.est.3c00537, 2023.

Seltzer, K. M., Pennington, E., Rao, V., Murphy, B. N., Strum, M., Isaacs, K. K., and Pye, H. O. T.: Reactive organic carbon emissions from volatile chemical products, Atmospheric Chem. Phys., 21, 5079–5100, https://doi.org/10.5194/acp-21-5079-2021, 2021.

Shang, Y., Chen, W., Bao, Q., Yu, Y., Pang, X., Zhang, Y., Guo, L., Fu, J., and Feng, W.: Characteristics and source profiles of atmospheric volatile organic compounds (VOCs) in the heavy industrial province of Northeast China with cruise monitoring, Front. Environ. Sci., 10, https://doi.org/10.3389/fenvs.2022.1055886, 2022.

Sinha, V., Williams, J., Crowley, J. N., and Lelieveld, J.: The Comparative Reactivity Method – a new tool to measure total OH Reactivity in ambient air, Atmospheric Chem. Phys., 8, 2213–2227, https://doi.org/10.5194/acp-8-2213-2008, 2008.

Spinelle, L., Gerboles, M., Kok, G., Persijn, S., and Sauerwald, T.: Review of Portable and Low-Cost Sensors for the Ambient Air Monitoring of Benzene and Other Volatile Organic Compounds, Sensors, 17, 1520,

https://doi.org/10.3390/s17071520, 2017.

Tan, Z., Lu, K., Hofzumahaus, A., Fuchs, H., Bohn, B., Holland, F., Liu, Y., Rohrer, F., Shao, M., Sun, K., Wu, Y., Zeng, L., Zhang, Y., Zou, Q., Kiendler-Scharr, A., Wahner, A., and Zhang, Y.: Experimental budgets of OH, HO_2, and RO_2 radicals and implications for ozone formation in the Pearl River Delta in China 2014, Atmospheric Chem. Phys., 19, 7129–7150, https://doi.org/10.5194/acp-19-7129-2019, 2019.

Vermeuel, M. P., Novak, G. A., Kilgour, D. B., Claflin, M. S., Lerner, B. M., Trowbridge, A. M., Thom, J., Cleary, P. A., Desai, A. R., and Bertram, T. H.: Observations of biogenic volatile organic compounds over a mixed temperate forest during the summer to autumn transition, Atmospheric Chem. Phys., 23, 4123–4148, https://doi.org/10.5194/acp-23-4123-2023, 2023.

Wang, C., Yuan, B., Wu, C., Wang, S., Qi, J., Wang, B., Wang, Z., Hu, W., Chen, W., Ye, C., Wang, W., Sun, Y., Wang, C., Huang, S., Song, W., Wang, X., Yang, S., Zhang, S., Xu, W., Ma, N., Zhang, Z., Jiang, B., Su, H., Cheng, Y., Wang, X., and Shao, M.: Measurements of higher alkanes using NO^+ chemical ionization in PTR-ToF-MS: important contributions of higher alkanes to secondary organic aerosols in China, Atmospheric Chem. Phys., 20, 14123–14138, https://doi.org/10.5194/acp-20-14123-2020, 2020.

Wang, L., Lun, X., Wang, Q., and Wu, J.: Biogenic volatile organic compounds emissions, atmospheric chemistry, and environmental implications: a review, Environ. Chem. Lett., 22, 3033–3058, https://doi.org/10.1007/s10311-024-01785-5, 2024a.

Wang, R., Zhang, S., Xue, J., Guo, L., and Li, L.: Speciated VOCs emissions and ozone formation potential from on-road vehicles in North China Plain based on detailed and localized source profiles, Environ. Technol. Innov., 32, 103422, https://doi.org/10.1016/j.eti.2023.103422, 2023.

Wang, W., Yuan, B., Su, H., Cheng, Y., Qi, J., Wang, S., Song, W., Wang, X., Xue, C., Ma, C., Bao, F., Wang, H., Lou, S., and Shao, M.: A large role of missing volatile organic compound reactivity from anthropogenic emissions in ozone pollution regulation, Atmospheric Chem. Phys., 24, 4017–4027, https://doi.org/10.5194/acp-24-4017-2024, 2024b.

Wine, P. H., Kreutter, N. M., Gump, C. A., and Ravishankara, A. R.: Kinetics of hydroxyl radical reactions with the atmospheric sulfur compounds hydrogen sulfide, methanethiol, ethanethiol, and dimethyl disulfide, J. Phys. Chem., 85, 2660–2665, https://doi.org/10.1021/j150618a019, 1981.

Wohl, C., Li, Q., A. Cuevas, C., P. Fernandez, R., Yang, M., Saiz-Lopez, A., and Simó, R.: Marine biogenic emissions of benzene and toluene and their contribution to secondary organic aerosols over the polar oceans, Sci. Adv., https://doi.org/10.1126/sciadv.add9031, 2023.

Wu, C., Wang, C., Wang, S., Wang, W., Yuan, B., Qi, J., Wang, B., Wang, H., Wang, C., Song, W., Wang, X., Hu, W., Lou, S., Ye, C., Peng, Y., Wang, Z., Huangfu, Y., Xie, Y., Zhu, M., Zheng, J., Wang, X., Jiang, B., Zhang, Z., and Shao, M.: Measurement report: Important contributions of oxygenated compounds to emissions and chemistry of volatile organic compounds in urban air, Atmospheric Chem. Phys., 20, 14769–14785, https://doi.org/10.5194/acp-20-14769-2020, 2020.

Wu, Y., Huo, J., Yang, G., Wang, Y., Wang, L., Wu, S., Yao, L., Fu, Q., and Wang, L.: Measurement report: Production and

https://doi.org/10.5194/egusphere-2026-1204
Preprint. Discussion started: 11 March 2026

loss of atmospheric formaldehyde at a suburban site of Shanghai in summertime, Atmospheric Chem. Phys., 23, 2997–3014, https://doi.org/10.5194/acp-23-2997-2023, 2023.

Xie, Q., Chen, W., Yuan, B., Huangfu, Y., He, X., Wu, L., Liu, M., You, Y., Shao, M., and Wang, X.: Significant but Overlooked: The Role of Anthropogenic Monoterpenes in Ozone Formation in a Chinese Megacity, Environ. Sci. Technol., https://doi.org/10.1021/acs.est.5c00001, 2025.

Yan, X., Qiu, X., Yao, Z., Liu, J., and Wang, L.: Emissions of Oxygenated Volatile Organic Compounds and Their Roles in Ozone Formation in Beijing, Atmosphere, 15, 970, https://doi.org/10.3390/atmos15080970, 2024.

Yang, G., Huo, J., Wang, L., Wang, Y., Wu, S., Yao, L., Fu, Q., and Wang, L.: Total OH Reactivity Measurements in a Suburban Site of Shanghai, J. Geophys. Res. Atmospheres, 127, e2021JD035981, https://doi.org/10.1029/2021JD035981, 2022.

Yang, Y., Shao, M., Keßel, S., Li, Y., Lu, K., Lu, S., Williams, J., Zhang, Y., Zeng, L., Nölscher, A. C., Wu, Y., Wang, X., and Zheng, J.: How the OH reactivity affects the ozone production efficiency: case studies in Beijing and Heshan, China, Atmospheric Chem. Phys., 17, 7127–7142, https://doi.org/10.5194/acp-17-7127-2017, 2017.

Zhang, B., Hu, X., Yao, L., Wang, M., Yang, G., Lu, Y., Liu, Y., and Wang, L.: Hydroxyl radical-initiated aging of particulate squalane, Atmos. Environ., 237, 117663, https://doi.org/10.1016/j.atmosenv.2020.117663, 2020.

Zhang, Y., Xu, W., Zhou, W., Li, Y., Zhang, Z., Du, A., Qiao, H., Kuang, Y., Liu, L., Zhang, Z., He, X., Cheng, X., Pan, X., Fu, Q., Wang, Z., Ye, P., Worsnop, D. R., and Sun, Y.: Characterization of organic vapors by a Vocus proton-transfer-reaction mass spectrometry at a mountain site in southeastern China, Sci. Total Environ., 919, 170633, https://doi.org/10.1016/j.scitotenv.2024.170633, 2024.

Zheng, X. and Xie, S.: Differences in the key volatile organic compound species between their emitted and ambient concentrations in ozone formation, Atmospheric Chem. Phys., 25, 3807–3820, https://doi.org/10.5194/acp-25-3807-2025, 2025.

Zhou, J., Wang, W., Wang, Y., Zhou, Z., Lv, X., Zhong, M., Zhong, B., Deng, M., Jiang, B., Luo, J., Cai, J., Li, X.-B., Yuan, B., and Shao, M.: Intercomparison of measured and modelled photochemical ozone production rates: Suggestion of chemistry hypothesis regarding unmeasured VOCs, Sci. Total Environ., 951, 175290, https://doi.org/10.1016/j.scitotenv.2024.175290, 2024.